Available online at www.sciencedirect.com

SCIENCE DIRECT®

Tectonophysics 390 (2004) 205–216

TECTONOPHYSICS

www.elsevier.com/locate/tecto

Near real-time magnitude determination for large crustal earthquakes

Yih-Min Wu[a], Ta-liang Teng[b,*]

[a]*Central Weather Bureau, 64 kung-Yuan Road, Taipei, Taiwan ROC*
[b]*Southern California Earthquake Center, University of Southern California, Los Angeles, CA 90089-0740, USA*

Received 26 December 2001; received in revised form 20 January 2002; accepted 9 March 2004
Available online 27 August 2004

Abstract

We introduce an empirical method of near real-time, near-field magnitude determination for large (M>6.5) crustal earthquakes. Time integration over the strong shaking duration on the absolute values of the acceleration records is carried out for nearby stations surrounding many large earthquake sources in Taiwan. The integrated quantity, here denoted as total effective shaking, is used in a regression process to derive an empirical relationship for a quick Mw determination useful for a reliable real-time operation in earthquake rapid reporting and earthquake early warning systems (EWSs).

Keywords: Seismic hazard mitigation; Magnitude; Seismic early warning; Seismic rapid reporting

1. Introduction

A large earthquake may be excited by a propagating rupture or by jumping dislocations, and may have a source dimension on the order of 100 km or more. The larger the earthquake is, the heavier the loss potential will be. From the standpoint of seismic hazards mitigation, it is imperative for a seismic network to determine as quickly as possible the location and magnitude (therefore the shaking intensity) of a large earthquake in order to quickly assess the potential damage and to timely offset the shake-induced secondary hazards. For this purpose, the Central Weather Bureau Seismic Network (CWBSN) of Taiwan has instigated a Rapid Reporting System (RRS) (Teng et al., 1997; Wu et al., 1997, 2000), and an earthquake early warning system (EWS) has also been put into operation (Wu and Teng, 2002). These systems are quickly becoming one of the promising tools in earthquake loss mitigation. The RRS and EWS issue critical information (hypocenter, magnitude, and intensity) within about a minute or less after the event occurrence, and transmit the information to populated areas and other locations of sensitive facilities, particularly to the emergency response

* Corresponding author.
E-mail addresses: ym.wu@socmail.cwb.gov.tw (Y.-M. Wu), lteng@usc.edu (T. Teng).

0040-1951/$ - see front matter © 2004 Published by Elsevier B.V.
doi:10.1016/j.tecto.2004.03.029

agencies. As the CWBSN systems transmit this critical information to emergency response agencies, these agencies can then take appropriate response actions (some of which are pre-programmed) immediately after an earthquake has struck. These response measures include the dispatch of rescue missions to areas of likely heavy damage.

The rapid earthquake location is now a simple and essentially solved problem. With modern computer and software, a network can produce reasonable earthquake location within a fraction of a second as soon as a few of the P (and/or S) arrivals are received. In the case of the CWBSN, a given event can be located in about 0.1 s (Wu, 1999; Wu and Teng, 2002)

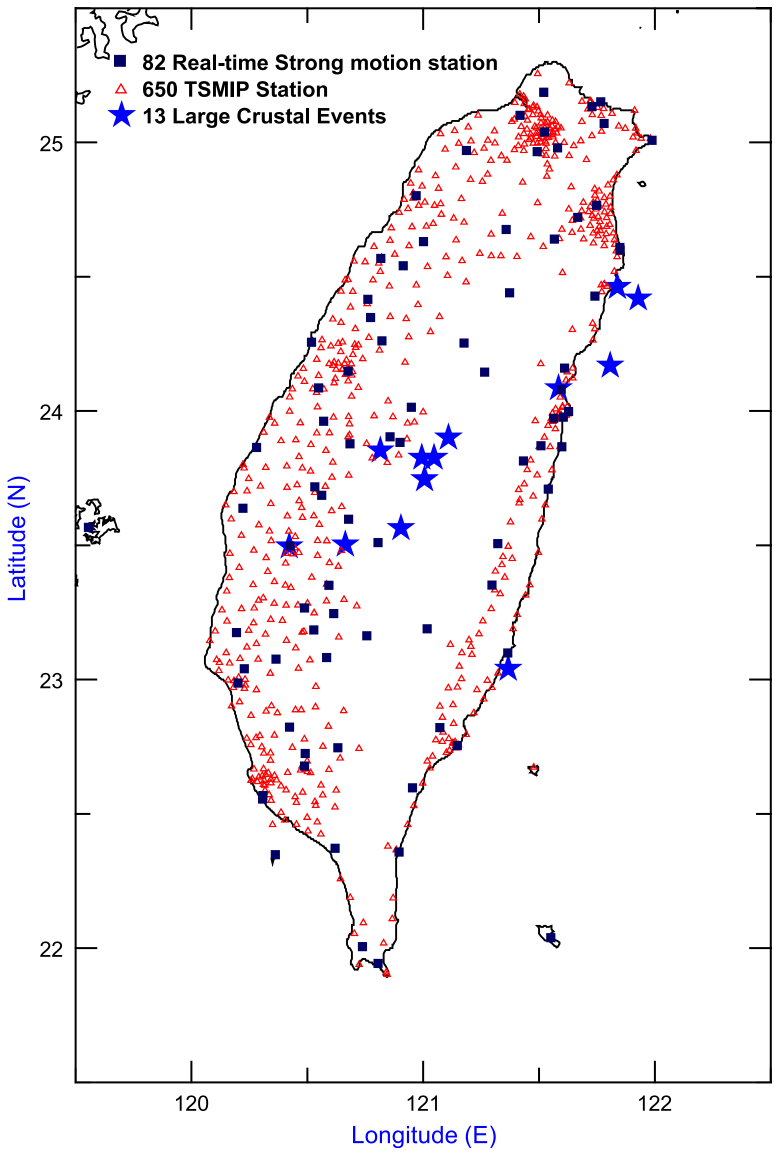

Fig. 1. Stations distribution of strong motion instruments in Taiwan. Stars show epicenters of the 13 large events used in this study. Solid square: 82 real-time telemetered strong-motion stations. Open triangle: 650 Taiwan free-field Strong-Motion Instrumentation Program (TSMIP) stations.

by a computer-configured virtual sub-network, which usually has a radius of about 50 km and for which the average P-wave travel-time is about 10 s or less. It is safe to say that for the CWBSN, the earthquake location computation is a 10-s problem and it is routinely accomplished (Wu et al., 1998, 1999).

However, a correct, quick measurement of the size (therefore the damage potential) of a large earthquake is a non-trivial problem. At teleseismic distance, a reasonably reliable moment magnitude *Mw* can be determined with global broadband recordings. Commonly, this *Mw* determination can only be done after waves have completed traversing the teleseismic wave paths, which can take tens of minutes—a length of time that is not acceptable to either RRS and EWS operations. At near-field distance, the wave travel-time is short. However, common high-gain broadband stations at this distance will severely saturate for large earthquakes and thus provide no means for *Mw* determination. Although Tsuboi et al. (1995, 1999) reported using broadband P waveforms to determine moment magnitude (*Mwp*) for the purpose of RRS. However, the reporting time still takes several minutes for moderate-sized earthquakes and a much longer time for big events. For extremely large earthquakes, at near-filed distances, because of large source dimensions, S waves from the early part of the rupture may interfere of even arrive before the P waves. It causes further difficulty and uncertainty of *Mwp* determination for such big events that are the main targets of RRS. The CWBSN has installed extensive telemetered strong-motion instruments using force-balanced sensors (FBAs), which basically have broadband response from DC to 50 Hz, 96 dB dynamic ranges and a 2-g saturation amplitude (Teng et al., 1997; Wu et al., 1997). Fig. 1 shows the current CWBSN 82 current real-time strong-motion stations (solid squares). Real-time on-scale recordings of waveforms of large events at near-field distances have become routinely available. However, the common *Mw* determination using near-field waveforms and a recursive moment tensor inversion routine still faces a difficulty which is largely due to the finiteness and complexity of a large propagating rupture. Thus, a thorough solution to the recursive moment tensor inversion problem will have to wait for the extension of the present theory to one for an extended finite complex rupture. In earlier papers (Wu et al., 2001; Wu and Teng, 2002), we have made attempts to look for an empirical relationship between M_L and *Mw*. While the CWBSN routinely determines M_L (Shin, 1993) using simulated Wood–Anderson seismograms (Kanamori et al., 1999) and a method developed by Richter (1935), we have found that for really large earthquakes ($M \geqslant 6.5$) the M_L scale saturate, and difficulties again arise preventing an adequate *Mw* determination. This paper introduces a practical empirical method that can quickly derive an equivalent *Mw* based on the real-time strong shaking waveforms.

Table 1
Parameters of 13 events used in this study

Origin time (UT)		Latitude (N)	Longitude (E)	Depth (km)	*Mw* (Harvard)	M_L	*Mew*
1994/06/05	01:09:30.09	24.462	121.838	5.3	6.3	6.20	6.25±0.29
1995/02/23	05:19:02.78	24.169	121.807	22.0	6.2	6.27	5.95±0.29
1995/05/27	18:11:11.12	23.040	121.367	22.0	5.7	5.60	5.68±0.36
1998/07/17	04:51:14.96	23.503	120.664	5.7	5.7	5.90	5.61±0.30
1999/09/20	17:47:15.85	23.853	120.815	8.0	7.6	7.06	7.59±0.26
1999/09/20	21:46:36.86	23.564	120.904	4.4	6.4	6.22	6.19±0.31
1999/09/22	00:14:40.77	23.826	121.047	15.6	6.4	6.47	6.56±0.26
1999/09/22	00:49:43.45	23.746	121.006	6.0	5.8	5.97	5.76±0.26
1999/09/25	23:52:47.28	23.826	120.994	20.9	6.5	6.44	6.49±0.35
1999/10/22	02:18:56.55	23.496	120.422	23.1	5.8	6.07	5.89±0.27
2000/06/10	18:23:29.45	23.901	121.109	16.2	6.4	6.52	6.53±0.30
2000/09/10	08:54:46.53	24.085	121.584	17.7	5.8	5.98	5.83±0.27
2001/06/14	02:35:25.78	24.419	121.928	17.6	5.9	6.23	5.89±0.38

2. Method and data

In this study, we shall describe our recently developed method for an *Mw* magnitude determination of large crustal earthquakes for RRS. We consider the total energy output in terms of strong shaking excited by a finite source area of large dimension (~100 km), knowing that the total energy may be the sum of energies from a large number of smaller sources (ruptures or dislocations) that may have occurred over several tens of seconds as the rupture proceeds. The method involves a time integration of the absolute values of strong ground acceleration of the near-field records. The integrated total strong shaking is then used to seek, through a regression analysis, an empirical relationship by correlating with input known values of *Mw.* At the same time, the regression analysis will determine the distance attenuation functions and the individual site correction factors as a refinement in the real-time empirical *Mw* determination.

Big and shallow earthquakes often cause serious damage in heavily populated areas. They are the most destructive events that a RRS is targeted at. Thus, we have assembled a large database of digital strong-motion records for 13 recent large crustal events in Taiwan for this study (Fig. 1 and Table 1). The selection criteria are $Mw \geq 5.7$ and focal depth <35 km, with the largest event being the 1999 *Mw* 7.6 Chi-Chi earthquake. All events were well recorded by stations of the Taiwan Strong Motion Instrumentation Program (TSMIP) network (triangles in Fig. 1). These large events used here occurred during 1994–2001 and were widely felt in Taiwan. A total of 2506 TSMIP records are used in this study. A typical data trace is shown in part A of Fig. 2. It is the east–west component record of the Chi-Chi earthquake mainshock taken at the station TCU078 at an epicentral distance of 5.5 km. The peak amplitude of 440 gal is seen. The total strong-shaking duration of this *Mw*7.6 event is about 30 s. Of particular interest are two features of the waveform that may illustrate the nature of strong shaking of large earthquakes:

(1) The first few seconds of the waveform represents the P (and perhaps also S) energy burst from a small nucleation event. From the waveform of these first few seconds, there is absolutely no information to indicate that this small nucleation event will or will not escalate into a large earthquake. It is therefore apparent that, regardless of what we do on the waveforms of these first few seconds (e.g., by examining the P-wave period and spectrum, etc.), we are not likely to get reliable magnitude information of the subsequent large event, which may or may not follow the initial nucleation rupture.

(2) The entire 30-s waveform here consists of a number of large energy bursts, indicating a number of major dislocations or ruptures of strong asperities over the entire rupture surface. Clearly, a really large event, like Chi-Chi, may

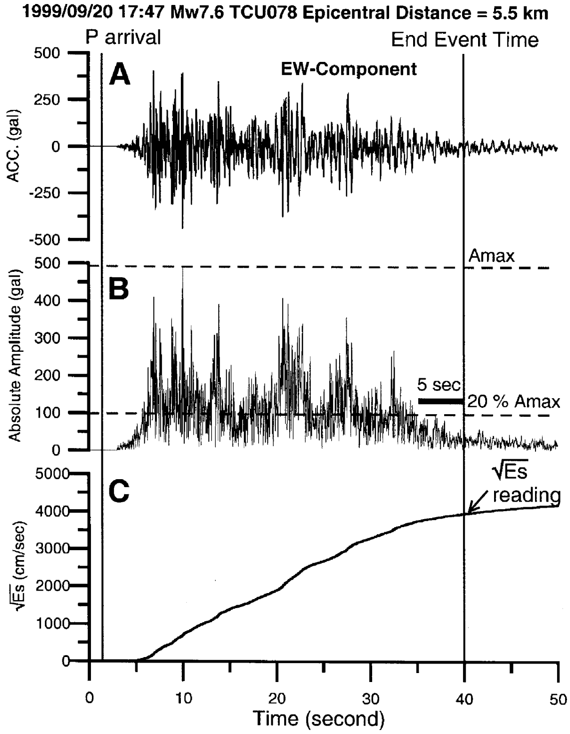

Fig. 2. A sample strong-motion records using in our analysis: (A) The EW component strong motion signal from the TSMIP station TCU078 for the 1999/09/20 17:47 *Mw* 7.6 Chi-Chi, Taiwan earthquake, recorded at 5.5 km from nearest point on the rupture. (B) The absolute amplitude computed from the three-component data. (C) The integrated *Es* values determined in this study. Also shown are in (B) the maximum amplitude (A_{max}) and the definition of end-of-event time (the vertical line at about 40 s mark). See text for details.

> neither be produced by a single simultaneous rupture of large dimensions, nor by a smoothly propagating finite rupture. For a large earthquake source with large dimensions, the occurrence of large energy bursts can normally be irregular both in space and time.

Therefore, to extract useful magnitude information from these near-field seismograms surrounding the source, one will have to deal with the total effective shaking embodied in the wave trains. This total effective shaking is proportional to the energy input into the medium from the source. From the hazard mitigation perspective in a RRS operation, we consider this total effective shaking to be a practical measure for the earthquake magnitude. We shall use this large data set to derive a reliable empirical method for *Mw* determination, specifically aiming at large events in a real-time monitoring operation.

3. Data analysis and results

To compute the total effective shaking embodied in the waveforms of the near-field acceleration

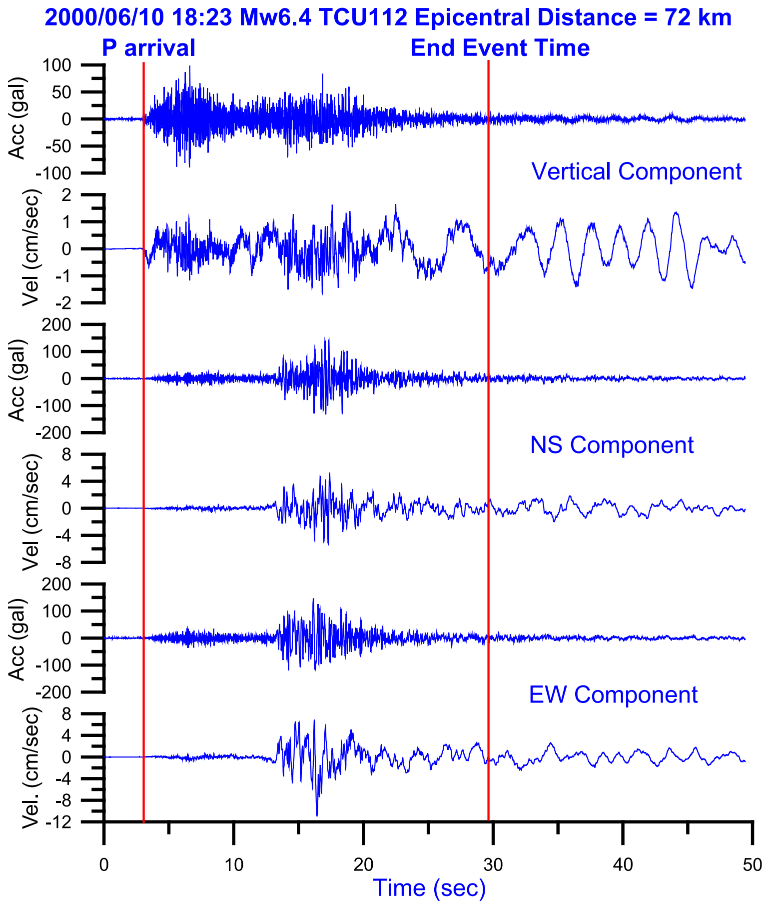

Fig. 3. Examples showing the differences in waveforms between the acceleration and velocity record for the TSMIP station TCU112 for event at 2000/06/10 18:23 *Mw* 6.4 recorded at 72 km away. Three sets of traces are shown for the vertical, NS, and EW components: with upper trace being acceleration, and lower trace being velocity. The vertical end-of-time line is at about 30 s. It demonstrates that for stations away from the source and located in basin geology, the excited long-period surface waves will make the search of end-of-event time difficult in an automated network monitoring operation.

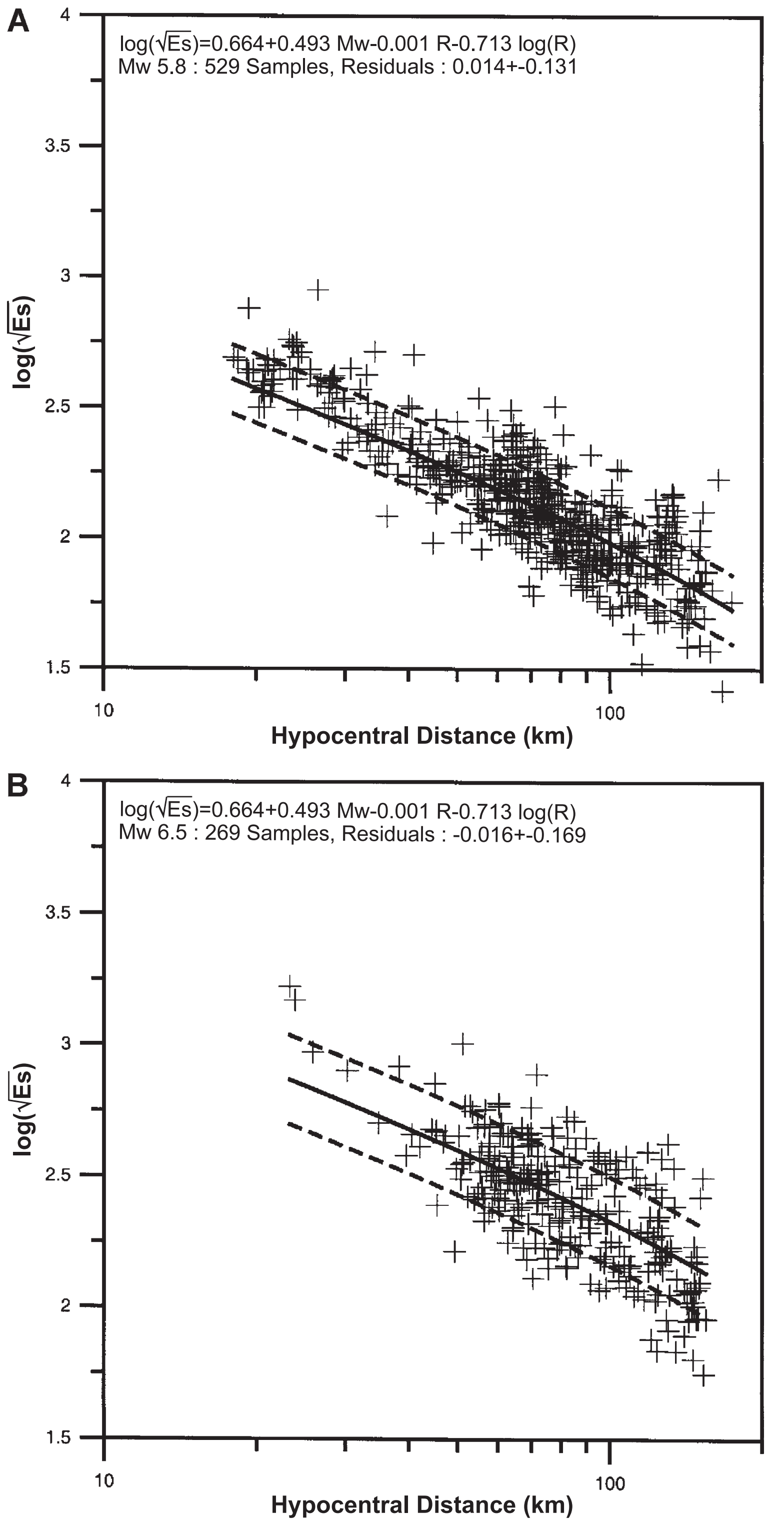
A
log(√Es)=0.664+0.493 Mw-0.001 R-0.713 log(R)
Mw 5.8 : 529 Samples, Residuals : 0.014+-0.131
log(√Es)
4
3.5
3
2.5
2
1.5
10
100
Hypocentral Distance (km)
B
log(√Es)=0.664+0.493 Mw-0.001 R-0.713 log(R)
Mw 6.5 : 269 Samples, Residuals : -0.016+-0.169
log(√Es)
4
3.5
3
2.5
2
1.5
10
100
Hypocentral Distance (km)

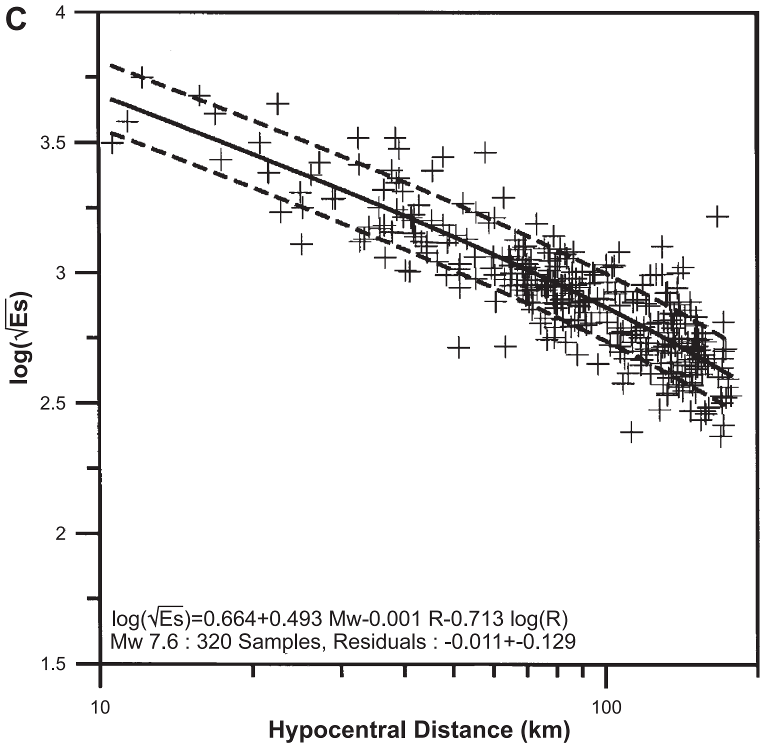

Fig. 4. (A) The regression solid curve, with one standard deviation dashed curves, is plotted against the integrated values of $\sqrt{Es}$ for an *Mw* 5.8 event. (B) The regression solid curve and one standard deviation dashed curve are plotted against the integrated values of $\sqrt{Es}$ for an *Mw* 6.5 event. (C) The regression solid curve and one standard deviation dashed curves are plotted against the integrated values of $\sqrt{Es}$ for an *Mw* 7.6 event.

recordings, we define an absolute-value acceleration integral $\sqrt{Es}$ such that:

$$\sqrt{Es} = \int_{T_p}^{T_e} \sqrt{V^2 + N^2 + E^2}\mathrm{d}t \qquad (1)$$

Here *V*, *N*, and *E* are vertical, north–south, and east–west components acceleration signals (in gal). The integrand gives the absolute amplitude *A* of the vector sum of the three-component accelerations. Upon integration, $\sqrt{Es}$ will have the unit of velocity, thus, *Es* is proportional to wave energy. T_p is the P-wave arrival time. T_e is the end-of-event time of the strong-shaking duration, which is defined as the point of time when the acceleration amplitude *A* drops below 20% of the maximum amplitude (A_{max}) and remains there for 5 s. The unit of T_p and T_e are in seconds. In part B of Fig. 2, A_{max} is shown to be close to 500 gal. The end-of-event time T_e occurs at about 40 s after the first P arrival, which is defined to be the time when *A* has become 20% of A_{max} for more than 5 s. Part C of Fig. 2 shows $\sqrt{Es}$, the total effective shaking, that builds up as the strong-shaking continues. The integration is cut off at 40 s for this case. The early cutoff is mainly for the interest of quickly completing the total effective shaking calculation so that the system can get on with the magnitude determination for the purpose of RRS. Indeed, after 40 s for this example, the additional increment of wave energy is small and can be neglected for the present purpose of *Mw* determination.

Here, we explain our choice of using acceleration records instead of velocity records for getting $\sqrt{Es}$. In Fig. 3, acceleration records (Station TCU112) for an *Mw* 6.4 event are shown for all three components. The corresponding integrated velocity record is shown below each acceleration record. We see that as the rupture process is coming to an end at about 20 s after the P arrival, the acceleration amplitudes substantially die off, yet, the velocity records sometimes show large-amplitude, low-frequency waves. These low-frequency waves can come from two sources: one being the excitation of surface waves in a sedimentary basin due to multiple reflections, the second being the accumulated integration errors due largely to the long-period noise. In either case, these low-frequency waves should not be included in the effective total shaking calculation. Furthermore, in real-time network data processing, it is easier to define the end-of-event time for acceleration records but not so for velocity records. Therefore, we choose to use acceleration records for our purpose.

The decrease in the amplitude of seismic waves with distance from the hypocenter can be represented by $Amp{\sim}e^{-\gamma R}/R^n$, where R is the hypocentral distance, n is geometrical spreading coefficient, and γ can be related to the anelastic attenuation coefficient Q. The magnitude is proportional to $\log(Amp)$; and $\log(Amp)$ can be expressed by $n\log(R)-(\gamma/\ln 10)R$+Cs; here, Cs is constant. In this study, $\sqrt{Es}$ is used as the acceleration amplitude integral. Thus, we consider the linear regression model as follows:

$$\log\left(\sqrt{Es}\right) = A + B{\cdot}Mw + C{\cdot}R + D{\cdot}\log(R) + S_i \quad (2)$$

Here, S_i is the ith site correction factor. The TSMIP station site amplification factors of peak ground acceleration (PGA) were determined in a previous study (Wu et al., 2001). Thus, here, S_i can be determined for each known site as the amplification factor. The coefficients A, B, C, and D are to be determined by least-squares regression. With a total of 2506 TSMIP records as the input, the resulting attenuation relationship for $\sqrt{Es}$ is given by

$$\log\left(\sqrt{Es}\right) = 0.664 + 0.493{\cdot}Mw - 0.001R - 0.713{\cdot}\log(R) + S_i \quad (3)$$

where $\log(\sqrt{Es})$ has approximately a normal distribution about the mean, and the standard deviation is

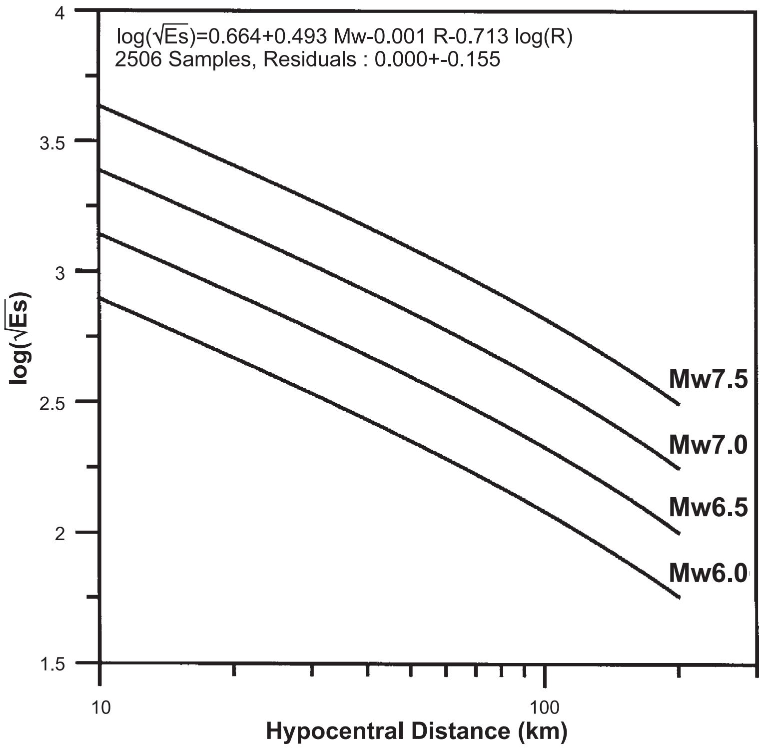

Fig. 5. Regression curves of $\sqrt{Es}$ for Mw=6.0, 6.5, 7.0, and 7.5.

0.155. It is interesting that *Mw* is given approximately by the value of log(*Es*). The comparisons between the observed and predicted $\sqrt{Es}$ values for *Mw* 5.8, 6.5, and 7.6 are shown in Fig. 4A, B, and C. From the entire data set, we can generate a set of regression curves, one useful set of curves for *Mw* 6.0, 6.5, 7.0, and 7.5 are given in Fig. 5. With the set of empirical curves derived, the CWBSN can practically determine near real time for any large Taiwan earthquake an equivalent *Mw* value as soon as a number of near-field waveforms are captured up to their end-of-event times for the strong shaking. This magnitude determination for large earthquakes will not have a saturation problem and can be carried out by the CWBSN in about 30 s to 1 min, which, although too slow for EWS, is quite adequate for the purpose of RRS.

4. Discussions

For real-time seismic monitoring, especially for RRS operation, near-field magnitude determination for large earthquakes is an outstanding problem. Clearly, the *Mw* determined by teleseismic broadband recordings will not meet the RRS time requirement. Near-field high-gain seismographs will have severe amplitude-clipping problem from which no useful waveform can help the *Mw* determination. One compromise is the use of the low-gain, large dynamic broadband system. The strong-motion FBAs, such as those TSMIP telemetered instruments installed by the CWBSN, ideally fit the requirements. This installation gives rise to a quick advancement of the RRS operation as reported here. The set of curves presented in Fig. 5 cover all large earthquakes that can be expected in Taiwan. They are derived here based on a large data set consisting of 2506 strong-motion records from 13 largest Taiwan crustal events. The strong-motion site amplification and attenuation data derived from recent large earthquakes are also incorporated into the magnitude calculation. All these data are recorded by the 650-station TSMIP network (Fig. 1, open triangles).

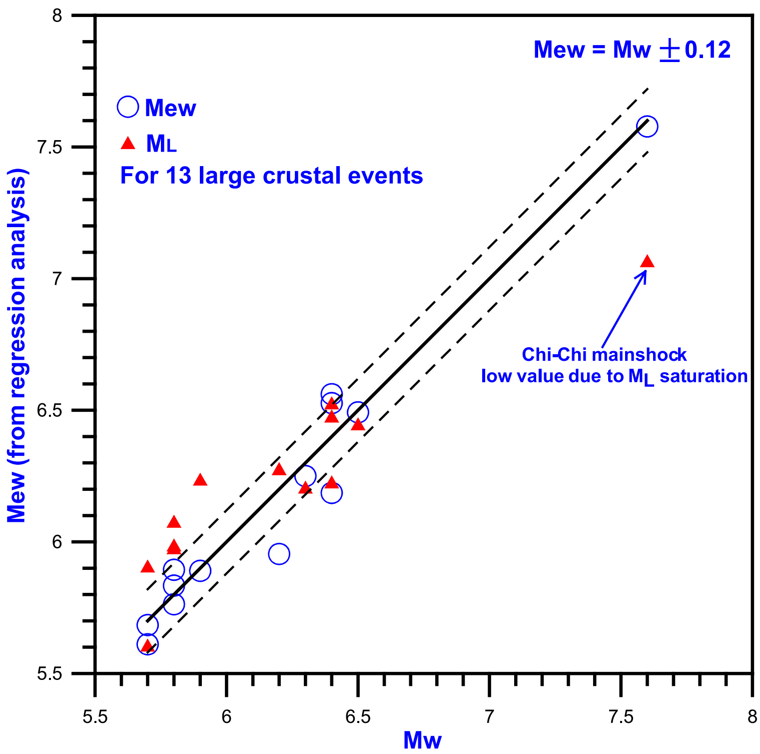

Fig. 6. The *Mew* and M_L data as plotted again a 45° line of *Mew*=*Mw*.

The set of empirical curves in Fig. 5 will allow a real-time equivalent *Mw* determination as soon as the waveform data for the strong shaking period is recorded. Since it only involves an integration of the absolute acceleration amplitude and an interpolation on the set of existing curves, the principal time needed is essentially the time to complete the recording of the strong shaking waveforms, i.e., about less than 1 min typically.

From this study, the log(*Es*) is found to be proportional to *Mw* in a simple manner; we shall rewrite Eq. (3) replacing *Mw* by *Mew* to reflect that a different process is used in moment magnitude derivation:

$$Mew = -1.347 + 1.014 \cdot \log(Es) + 0.002 \cdot R + 1.446 \cdot \log(R) - 2.0258 \cdot S_i \quad (4)$$

Here, *Mew* is derived empirically through an integration process by summing up the earthquake strong shaking absolute amplitude. The integrated quantity has a unit of velocity, which bears a simple relation to the total energy, in fact, log(*Es*)~*Mew*.

In Table 1, we listed the values of *Mw* (from teleseismic data), M_L (from CWBSN), and *Mew* with error bars (from this study). Fig. 6 gives a comparison of the three magnitude values by plotting the *Mew* against a 45° *Mew*=*Mw* line, with the dashed lines giving one standard deviation values. The figure shows that M_L values (in solid triangles) are scattered about the 45° *Mew*=*Mw* line, and give a significantly lower value for the large Chi-Chi *Mw* 7.6 event due to M_L saturation. The *Mew* values stay mostly well inside one standard deviation. The *Mew* value for the large Chi-Chi *Mw* 7.6 event falls almost right on the mark with a standard deviation of 0.12. The differences between *Mew* and *Mw* are distributed in a small range from −0.25 to 0.16. This result shows the magnitude of large crustal earthquakes in Taiwan can be well determined from $\sqrt{Es}$, or from an integration of absolute amplitude over the strong shaking period.

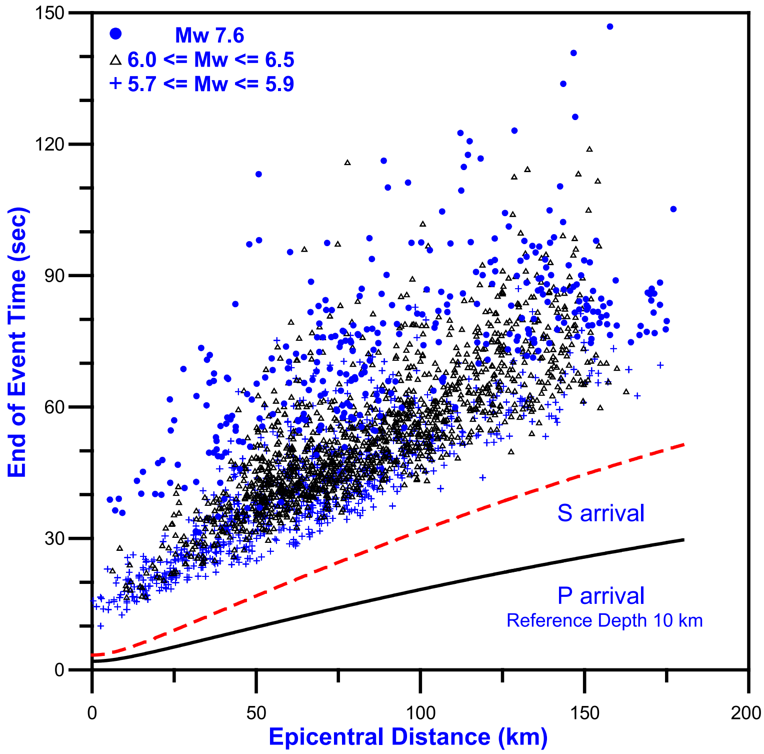

Fig. 7. Distribution of the end-of-event times for 2506 records used in this study.

This integration is fast and can be carried out in real time. Therefore, the *Mew* determination is practical in the RRS operation.

Fig. 7 shows data of the end-of-event times of the 2506 records used in this study. Except for the Chi-Chi mainshock, most of the end-of-event times have values between 15 and 30 s after the S-wave arrival. The end-of-event times of the Chi-Chi mainshock lasted more than 30 s after the S-wave arrivals, especially at large distances. For large earthquakes like the Chi-Chi event, one should expect large ruptures (100×40 km) and long rupture times (~30 s). Even then, in a typical RSS operation, with a dense real-time strong-motion station network as shown in Fig. 1, only stations with epicentral distances less than 60 km are involved in the $\sqrt{Es}$ calculation. The method presented here still can produce a reliable *Mew* (therefore an equivalent *Mw*) within about 1 min.

5. Conclusions

In real-time seismic monitoring for an earthquake RSS, we have obtained a method that can deliver the value *Mew* (therefore an equivalent value of *Mw*) mainly for large on-land earthquakes. Future data may justify an extension of this method to be applied to subduction earthquakes that occur offshore of east Taiwan. Due to the greater depth and larger distance, these subduction earthquakes are far less damaging to centers of population on Taiwan's west coast. This method avoids the magnitude saturation problem caused in the M_L determination for large events, and significantly speed up the delivery of an equivalent *Mw* values normally come from teleseismic broadband recordings. The teleseismic *Mw* determination, of course, is too late for the RRS. We have achieved this by an integration of the total ground shaking $\sqrt{Es}$ and have derived an empirical relationship between *Mw* and *Mew*, which bears a simple relationship with the easily computed $\log(\sqrt{Es})$, i.e., $\log(Es)$~*Mew*~*Mw.* With this new method, *Mw* can be determined from *Mew* with a small uncertainty of 0.12. We shall use *Mew,* instead *Mw,* to identify this new magnitude that is determined from integrating the strong motion signals. It can be obtained reliably in less that 1 min and should prove to be useful for earthquake rapid reporting in real-time earthquake monitoring. With near real-time data from the 82 telemetered strong-motion stations, any earthquake rapid reporting information package also includes the acceleration $A(t)$, velocity $V(t)$ as well as the intensity map.

Acknowledgments

We wish to thank Dr. Steve Harmsen and an anonymous reviewer for comments and suggestions that greatly help improve this work. This work was supported by the Central Weather Bureau and the National Science Council of the Republic of China under Grant No. NSC91-2116-M-052-001 and MOTC-CWB-93–E-05. The author (TLT) was also supported by NSF Grant No. EAR-0001016.

References

Kanamori, H., Maechling, P., Hauksson, E., 1999. Continuous monitoring of ground-motion parameters. Bull. Seismol. Soc. Am. 89, 311–316.

Richter, C., 1935. An instrumental earthquake magnitude scale. Bull. Seismol. Soc. Am. 25, 1–32.

Shin, T.C., 1993. The calculation of local magnitude from the simulated Wood–Anderson seismograms of the short-period seismograms. TAO 4, 155–170.

Teng, T.L., Wu, Y.M., Shin, T.C., Tsai, Y.B., Lee, W.H.K., 1997. One minute after: strong-motion map, effective epicenter, and effective magnitude. Bull. Seismol. Soc. Am. 87, 1209–1219.

Tsuboi, S., Abe, K., Takano, K., Yamanaka, Y., 1995. Rapid determination of Mw from broadband P waveforms. Bull. Seismol. Soc. Am. 83, 606–613.

Tsuboi, S., Whitmore, P.M., Sokolowski, T.J., 1999. Application of Mwp to deep and teleseismic earthquakes. Bull. Seismol. Soc. Am. 83, 606–613.

Wu, Y.M., 1999. Development of event location software in an earthquake rapid reporting system. Central Weather Bureau Research and Development Report CW88-1A-08. 58 pp.

Wu, Y.M., Teng, T.L., 2002. A virtual subnetwork approach to earthquake early warning. Bull. Seismol. Soc. Am. 92, 2008–2018.

Wu, Y.M., Chen, C.C., Shin, T.C., Tsai, Y.B., Lee, W.H.K., Teng, T.L., 1997. Taiwan rapid earthquake information release system. Seismol. Res. Lett. 68, 931–943.

Wu, Y.M., Shin, T.C., Tsai, Y.B., 1998. Quick and reliable determination of magnitude for seismic early warning. Bull. Seismol. Soc. Am. 88, 1254–1259.

Wu, Y.M., Chung, J.K., Shin, T.C., Hsiao, N.C., Tsai, Y.B., Lee, W.H.K., Teng, T.L., 1999. Development of an integrated seismic early warning system in Taiwan—case for the Hualien area earthquakes. TAO 10, 719–736.

Wu, Y.M., Lee, W.H.K., Chen, C.C., Shin, T.C., Teng, T.L., Tsai, Y.B., 2000. Performance of the Taiwan rapid earthquake information release system (RTD) during the 1999 Chi-Chi (Taiwan) earthquake. Seismol. Res. Lett. 71, 338–343.

Wu, Y.M., Shin, T.C., Chang, C.H., 2001. Near real-time mapping of peak ground acceleration and peak ground velocity following a strong earthquake. Bull. Seismol. Soc. Am. 91, 1218–1228.